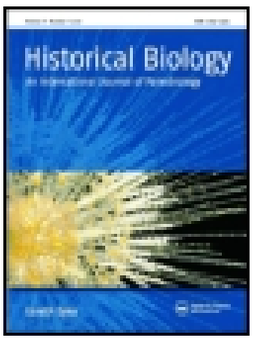

Historical Biology

An International Journal of Paleobiology

ISSN: (Print) (Online) Journal homepage: https://www.tandfonline.com/loi/ghbi20

The morphology and function of the manual digits of a troodontid from the Yixian Formation of western Liaoning, China

Dongxiang Yu, Rui Pei, Ya-Lei Yin & Chang-Fu Zhou

To cite this article: Dongxiang Yu, Rui Pei, Ya-Lei Yin & Chang-Fu Zhou (2022): The morphology and function of the manual digits of a troodontid from the Yixian Formation of western Liaoning, China, Historical Biology, DOI: 10.1080/08912963.2022.2155149

To link to this article: https://doi.org/10.1080/08912963.2022.2155149

Published online: 15 Dec 2022.

HISTORICAL BIOLOGY
https://doi.org/10.1080/08912963.2022.2155149

Taylor & Francis
Taylor & Francis Group

The morphology and function of the manual digits of a troodontid from the Yixian Formation of western Liaoning, China

Dongxiang Yu[a], Rui Pei[b,c], Ya-Lei Yin[d] and Chang-Fu Zhou[a]

[a]College of Earth Science and Engineering, Shandong University of Science and Technology, Qingdao, China; [b]Key Laboratory of Evolutionary Systematics of Vertebrates, Institute of Vertebrate Paleontology and Paleoanthropology, Chinese Academy of Sciences, Beijing, China; [c]CAS Center for Excellence in Life and Paleoenvironment, Beijing, China; [d]College of Palaeontology, Shenyang Normal University, Shenyang, China

ABSTRACT

A well-preserved paravian manus was described from the Jehol Biota of western Liaoning, China. This specimen was inferred as an early-diverging troodontid and reveals new morphological details of the troodontid clade, such as both ends of phalanx II-1 and phalanx II-2 asymmetrical, phalanx II-1 and phalanx III-3 twisted medially, the ventral side of the distal end of phalanx II-2 flat, and the proximal articular surface of phalanx III-1 non-trochoid. The range of motion of this manus was examined based on the CT data of the bones, showing that the range of flexion of this troodontid manus is relatively large while the range of extension is relatively limited, which is consistent with the tendency of the decrease in the manual extension capabilities from early-diverging theropods to maniraptoriforms.

ARTICLE HISTORY
Received 28 September 2022
Accepted 1 December 2022

KEYWORDS
Jehol Biota; Troodontidae; manual digits; morphology; function

Introduction

Troodontidae is a clade of middle to small bodied theropod dinosaurs and is widely distributed in Asia, Europe and North America (Makovicky and Norell 2004; Tsuihiji et al. 2014; Evans et al. 2017). Troodontids are considered as one of the closest relatives of birds (Agnolin et al. 2019; Rauhut and Foth 2020). In the last three decades, the northern China and southern Mongolia have yielded many troodontid fossils, which revealed abundant skeletal details of this clade and greatly improved our understanding of the transition from non-avialan dinosaurs to birds (Russell and Dong 1993; Norell et al. 2000; Xu et al. 2002, 2011, 2017; Xu and Norell 2004; Xu and Wang 2004; Ji et al. 2005; Gao et al. 2012a; Tsuihiji et al. 2014; Shen et al. 2017a, 2017b; Pei et al. 2017a, 2022; Yin et al. 2018). However, the morphology and the function of the forelimbs, especially the manus of troodontids, are understudied due to the lack of well-preserved or well-exposed materials. Only few troodontid manus were described in detail (Currie and Dong 2001; Averianov and Sues 2016; Tsuihiji et al. 2016). Here we provide a comprehensive description of a recently discovered troodontid manus from the Lower Cretaceous Yixian Formation of western Liaoning, China, based on three-dimensional reconstruction of CT-scan data and estimate the range of motion (ROM) of the digits.

The ROM analysis of the manus has been performed in many theropod taxa, including the basal theropods *Coelophysis bauri* (Carpenter 2002), *Dilophosaurus wetherilli* (Senter and Sullivan 2019), *Herrerasaurus ischigualastensis* (Sereno 1993) and *Megapnosaurus rhodesiensis* (Galton 1971), the allosauroids *Acrocanthosaurus atokensis* (Senter and Robins 2005) and *Allosaurus fragilis* (Carpenter 2002), the tyrannosauroids *Australovenator wintonensis* (its phylogenetic placement is still ambiguous in Tyrannosauroidea, White et al. 2015), *Guanlong wucaii* (Yu et al. 2015) and *Tyrannosaurus rex* (Carpenter 2002), the ornithomimosaurians *Deinocheirus mirificus* (Osmólska and Roniewicz 1969), *Gallimimus* sp. (Kobayashi and Barsbold 2005), *Harpymimus okladnikovi* (Kobayashi and Barsbold 2005) and *Ornitholestes hermanni* (Senter 2006a), the oviraptorosaurian *Chirostenotes pergracilis* (Senter and Parrish 2005), the dromaeosaurids *Bambiraptor feinbergi* (Senter 2006b) and *Deinonychus antirrhopus* (Gishlick 2001; Carpenter 2002; Senter 2006b). As in the previous studies (Senter and Robins 2005; Senter 2006b; White et al. 2015; Yu et al. 2015; Senter and Sullivan 2019), the bone-on-bone method is used to estimate the ROM, which ignores the influence of cartilages on the joint movement. Although the precise estimation of the ROM requires considering the interaction between bones and cartilages, the accurate reconstruction of cartilaginous epiphyses is unachievable at the current stage due to soft tissues are mostly unpreserved in the fossils (White et al. 2015).

Material and methods

SDUST-V1042 (Figures 1–4) was discovered from the Lower Cretaceous Yixian Formation at Lujiatun, Beipiao, western Liaoning, China. This specimen is represented by an articulated and 3d preserved right manus. Most manual digits of SDUST-V1042 are completely preserved. Metacarpals II and III and phalanx I-1 are preserved only with the distal ends, while metacarpal I is missing in this specimen.

This specimen was CT-scanned at China University of Geosciences (Beijing) using Nikon XT H225 ST (149 kV, 56 μA) and a total of 3143 slices were generated. A single pixel is 2000 × 2000 and each frame is 40 μm. The slices were imported into VG Studio MAX 3.0 (Volume Graphics, Heidelberg, Germany) for three-dimensional reconstruction. Surface measurements were performed on the three-dimensional model. The generated STL files were imported into Maya (Autodesk, California, USA) for the ROM analysis.

As in previous studies (Carpenter 2002; Kobayashi and Barsbold 2005; Senter and Robins 2005; Senter 2006a, 2006b; White et al.

CONTACT Rui Pei peirui@ivpp.ac.cn; Chang-Fu Zhou zhoucf528@163.com Key Laboratory of Evolutionary Systematics of Vertebrates, Institute of Vertebrate Paleontology and Paleoanthropology, Chinese Academy of Sciences, Beijing, China; Chang-Fu Zhou zhoucf528@163.com College of Earth Science and Engineering, Shandong University of Science and Technology, Qingdao, China

Published online 15 Dec 2022

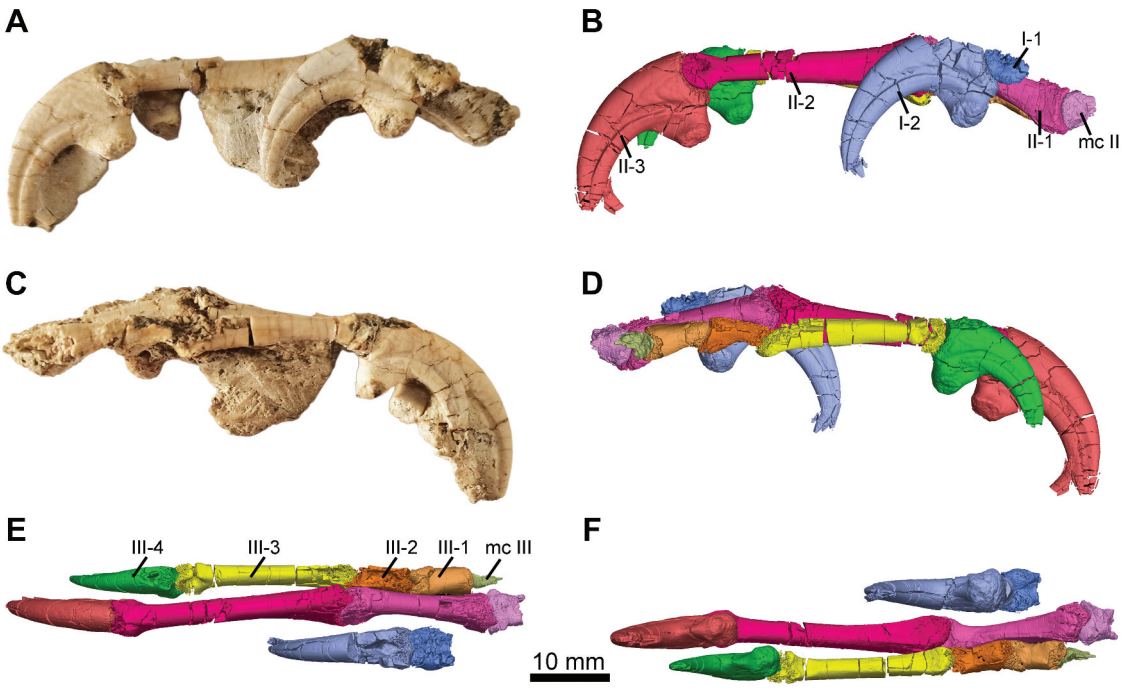

Figure 1. Photographs of SDUST-V1042 in medial (A) and lateral (C) views, and CT-rendered images of SDUST-V1042 in medial (B), lateral (D), dorsal (E) and ventral (F) views. Abbreviations: **I-1–I-2**, the phalanges of the manual digit I; **II-1–II-3**, the phalanges of the manual digit II; **III-1–III-4**, the phalanges of the manual digit III; **mcII–mcIII**, the metacarpals II and III.

2015; Senter and Sullivan 2019), the edges of the articular surfaces were assumed to represent the limits of motion; these limitations determined by the articular surface of the distal bone will reach but not move past the articular surface of the proximal bone. Maya was used to manipulate the phalanges to their ROM limits. A line was drawn down the long axis of each element, and the ranges of motion were measured from the angles between the lines. The long axis of each phalanx was considered as a line connecting the center of the distal condyle of the preceding phalanx to the center of the distal condyle of this phalanx. The long axis of each ungual was considered to be perpendicular to the line connecting the tips of the dorsal and ventral lips of the proximal articular surface of the ungual (Senter and Sullivan 2019). Phalanges I-1, I-2, II-1, II-2, II-3, III-1, III-2, III-3, III-4 are used for the ROM estimation (Figure 5). The ROM of digit I and the interphalangeal joint between phalanges III-2 and III-3 are estimated based on the incomplete joints.

Institution abbreviations

IGM, Institute of Geology, Ulaan Baatar, Mongolia (Ulaan Baatar, Mongolia); MPC, Mongolian Paleontological Center, Mongolian Academy of Sciences (Ulaan Baatar, Mongolia); SDUST, Vertebrate Palaeontological Collection of College of Earth Science and Engineering, Shandong University of Science and Technology (Qingdao, China).

Description

SDUST-V1042 (Figures 1–4) shows a phalangeal formula of 2-3-4. The manus is generally slender and well ossified. Digit II is longer than digit III, as typical for theropods. Phalanx II-2 is the longest preserved manual phalanx, while the length of phalanx I-1 is unknown.

The distal ends of metacarpals II and III are preserved (Figure 1). The distal end of metacarpal II consists of two asymmetrical condyles, with the lateral condyle larger than medial one (Figure 3e). Metacarpal III is articulated with the manual phalanx III-1.

The first manual digit is comprised of two phalanges (Figure 2). Phalanx I-1 is preserved with only a partial distal end (Figure 2). It consists of two condyles, subequal in size (Figure 2e).

The first ungual (phalanx I-2) is damaged at the proximodorsal portion and the distal tip (Figure 2). As in *Jianianhualong tengi* (Xu et al. 2017) and *Jinfengopteryx elegans* (Ji et al. 2005), the size of the first ungual is comparable to that of ungual of digit II. The first ungual is more curved than the second and third unguals. The proximal articular surface is divided by an inclined middle ridge (Figure 2f). The flexor tubercle is strongly developed, implying the presence of flexor muscles with good leverage (Ostrom 1969). The flexor tubercle is expanded transversely and nodule-like (Figure 2f). There is a circumferential shallow notch situated between the flexor tubercle and the proximal articular facet (Figure 2f). Distally, the flexor tubercle merges into the ventral margin of the ungual. On the lateral and medial surfaces, the ungual is sculptured by a distinct blood groove that tapers distally (Figure 2a, d).

The second manual digit is composed of three phalanges (Figures 1, 3). Phalanx II-1 (Figure 3) is well preserved with a length of 20 mm. As in *Liaoningvenator curriei* (Shen et al. 2017b) and *Mei long* (Gao et al. 2012a), this phalanx is slightly thicker than phalanx II-2 in diameter. However, in avialans such as *Confuciusornis sanctus* (Dalsätt et al. 2006), *Eoconfuciusornis zhengi* (Zhang et al. 2008) and *Jeholornis prima* (Zhou and Zhang 2002), phalanx II-1 is almost twice as thick as phalanx II-2 in diameter. The phalanx bears a well-developed ventral intercondylar tuberosity at the proximal end. The maximal dorsoventral height of the

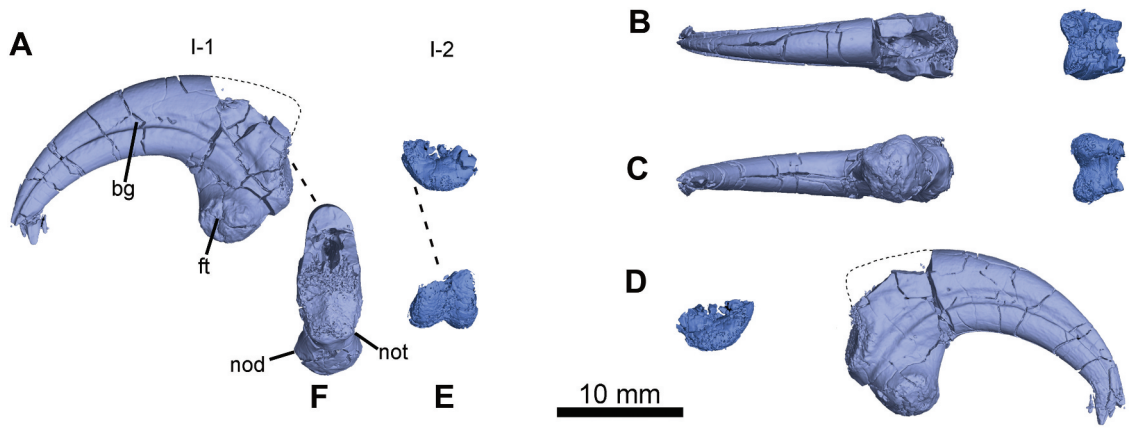

Figure 2. Manual digit I of SDUST-V1042 in medial (A), dorsal (B), ventral (C) and lateral (D) views; (E), distal view of phalanx I-1; (F), proximal view of phalanx I-2. Abbreviations: **bg**, blood groove; **ft**, flexor tubercle; **nod**, nodule; **not**, notch.

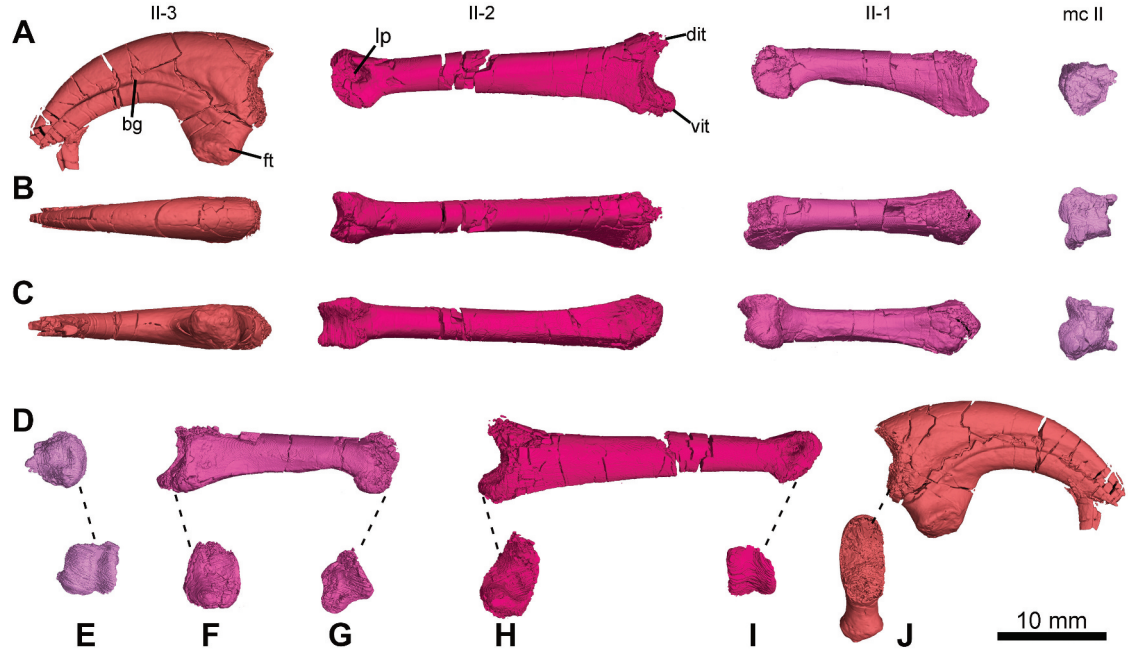

Figure 3. Manual digit II of SDUST-V1042 in medial (A), dorsal (B), ventral (C) and lateral (D) views; (E), distal view of metacarpal II; (F), proximal view of phalanx II-1; (G), distal view of phalanx II-1; (H), proximal view of phalanx II-2; (I), distal view of phalanx II-2; (J), proximal view of phalanx II-3. Abbreviations: **bg**, blood groove; **dit**, dorsal intercondylar tuberosity; **ft**, flexor tubercle; **lp**, ligament pit; **mc**, metacarpal; **vit**, ventral Intercondylar tuberosity.

bone is 5 mm at the proximal end. The proximal articular surface is divided and asymmetrical, with a larger lateral facet and a smaller medial facet (Figure 3f). The shaft is gradually reduced in thickness distally. It is oval in the cross section, with a diameter of about 3 mm at the mid-shaft. The shaft is slightly bowed ventrally. Notably, the shaft twists medially from its middle part, causing the distal end to flare medially (Figure 3g). The distal end of the phalanx is ginglymoid, and the lateral condyle is larger than the medial one (Figure 3g). In distal view, the ventral side of the lateral condyle expands laterally to form a small tubercle (Figure 3g). The distal condyles are subcircular in lateral view. No collateral ligament pit is developed at the distal end of the phalanx.

Phalanx II-2 is well preserved (Figure 3). It is 29 mm long. The proximal end is robust and with ventral and dorsal intercondylar tuberosities developed (Figure 3a), which limit the flexibility of the joint. As in phalanx II-1, the proximal articular surface is also divided into two asymmetrical facets, with the lateral facet larger than the medial one (Figure 3h). The mid-shaft diameter of the phalanx is about 2.5 mm. The cross section is rectangular at the proximal end and gradually becomes oval toward the distal end. The distal end is ginglymoid with two asymmetrical condyles (Figure 3i). The ventral side of lateral condyle is flat in lateral view (Figure 3d), while the medial condyle is rounded in medial view (Figure 3a). This flattening of the lateral condyle limits the hyperextension of phalanx II-3, as phalanx II-3 would become disarticulated with phalanx II-2 if hyperextended. Ligament pits are large and dorsally shifted on the lateral and medial faces of the distal articulation (Figure 3a, d), as in *Velociraptor mongoliensis* (Norell and Makovicky 1999), which is to prevent disarticulation of the phalanges of digit II (Ostrom 1969). Notably, the ligament pits are only present in phalanges II-2 and III-3 (Figures 3, 4), but absent or unpreserved in other phalanges.

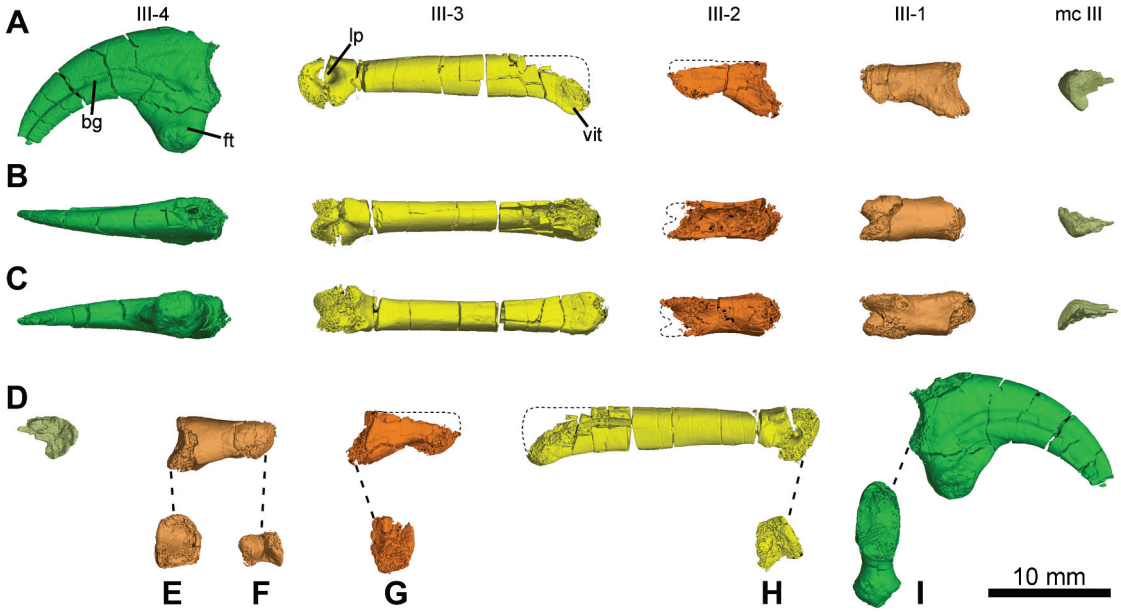

Figure 4. Manual digit III of SDUST-V1042 in medial (A), dorsal (B), ventral (C) and lateral (D) views; (E), proximal view of phalanx III-1; (F), distal view of phalanx III-1; (G), proximal view of phalanx III-2; (H), distal view of phalanx III-3; (I), proximal view of phalanx III-4. Abbreviations: **bg**, blood groove; **ft**, flexor tubercle; **lp**, ligament pit; **mc**, metacarpal; **vit**, ventral intercondylar tuberosity.

The second ungual (phalanx II-3) is nearly complete and only missing the distal tip (Figure 3). Proximally, the articular surface consists of two subequal facets, as in phalanx I-2. The flexor tubercle is significantly transversely expanded (Figure 3j). The dorsoventral height of the articular facet is slightly greater than that of the flexor tubercle. The proximodorsal lip is absent, as in *Jianianhualong tengi* (Xu et al. 2017) and *Mei long* (Gao et al. 2012a), but present in *Anchiornis huxleyi* (Pei et al. 2017b) and *Microraptor zhaoianus* (Xu et al. 2000; Gong et al. 2012; Pei et al. 2014). The blood groove is extended and positioned relatively dorsally along the lateral and medial surfaces (Figure 3a, d).

The third manual digit includes four phalanges (Figure 4). As in *Jianianhualong tengi* (Xu et al. 2017) and the unnamed troodontids (IGM 100/1126, Pei 2015; MPC-D 100/140, Tsuihiji et al. 2016), phalanges III-1 (9.5 mm) and III-2 (9.7 mm) are subequal in length, but shorter than phalanx III-3 (23 mm). This feature is common in troodontids, except that in *Sinornithoides youngi* phalanx III-2 appears twice as long as the III-1 (Currie and Dong 2001). Phalanges III-1, III-2 and III-3 bear ventral intercondylar tuberosities on the proximal ends (Figure 4a, d). The proximal articular surface of phalanx III-1 is non-trochoid (Figure 4e). This morphology implies that the third digit can move somewhat horizontally (adduction and abduction), as in *Acrocanthosaurus atokensis* (Senter and Robins 2005). The shaft of phalanx III-1 is circular in the cross section. The distal end of phalanx III-1 is ginglymoid, and the lateral condyle is slightly larger than the medial one (Figure 4f). Phalanx III-2 is comparable to phalanx III-1 in its form and size, and the proximal articular surface is also asymmetric (Figure 4g). Phalanx III-3 is elongated. Its mid-shaft is about 2 mm wide and oval in the cross section. The shaft also twists medially, as in phalanx II-1. Its distal end is ginglymoid with two nearly symmetrical condyles (Figure 4h). The condyles hardly expand dorsally, in contrast to those of phalanx II-2. The collateral ligament pits are large, and positioned relatively dorsally on both sides, as in phalanx II-2 (Figure 4a, d).

The third ungual (phalanx III-4) is also damaged at the proximodorsal portion and the distal tip (Figure 4). Phalanx III-4 is the smallest of all manual unguals. The morphology of the proximal articular facet, the flexor tubercle and the blood groove are similar to those of other unguals (Figure 4a,d,i).

Results

Taxonomic identification of SDUST-V1042

In the Jehol Biota, theropod fossils include tyrannosauroids, compsognathids, ornithomimosaurians, therizinosauroids, oviraptorosaurians, dromaeosaurids, troodontids and avialans. Among these theropod groups, SDUST-V1042 shows a high morphological resemblance to the early-diverging troodontids. Among the Jehol troodontids with preserved manus such as *Daliansaurus liaoningensis* (Shen et al. 2017a), *Jianianhualong tengi* (Xu et al. 2017), *Jinfengopteryx elegans* (Ji et al. 2005; Ji and Ji 2007) and *Mei long* (Xu and Norell 2004), the manual phalanges III-1 and III-2 are subequal in length and phalanx III-3 is longer than III-1 and III-2 combined, similar to SDUST-V1042. Moreover, SDUST-V1042 is similar to these Jehol troodontids based on other features such as the proximodorsal lip of phalanx II-3 absent, flexor tubercle strongly developed and subequal to the proximal articular facet in height, phalanx II-1 only slightly thicker than II-2 and shafts of digit II and digit III subequal in width. Furthermore, these shared features among SDUST-V1042 and other Jehol troodontids are also distributed in the manus of other troodontids (e.g. unnamed troodontids IGM 100/44, Barsbold et al. 1987 and MPC-D 100/140, Tsuihiji et al. 2016). For SDUST-V1042, further taxonomic identification within Troodontidae is difficult due to most of the skeleton of this specimen is not preserved.

SDUST-V1042 displays obvious differences from other theropods of the Jehol Biota. In tyrannosauroids such as *Dilong paradoxus* (Xu et al. 2004) and *Yutyrannus huali* (Xu et al. 2012), digit III is extremely slender and much narrower than digit II, but in SDUST-V1042, the width of digit III is similar

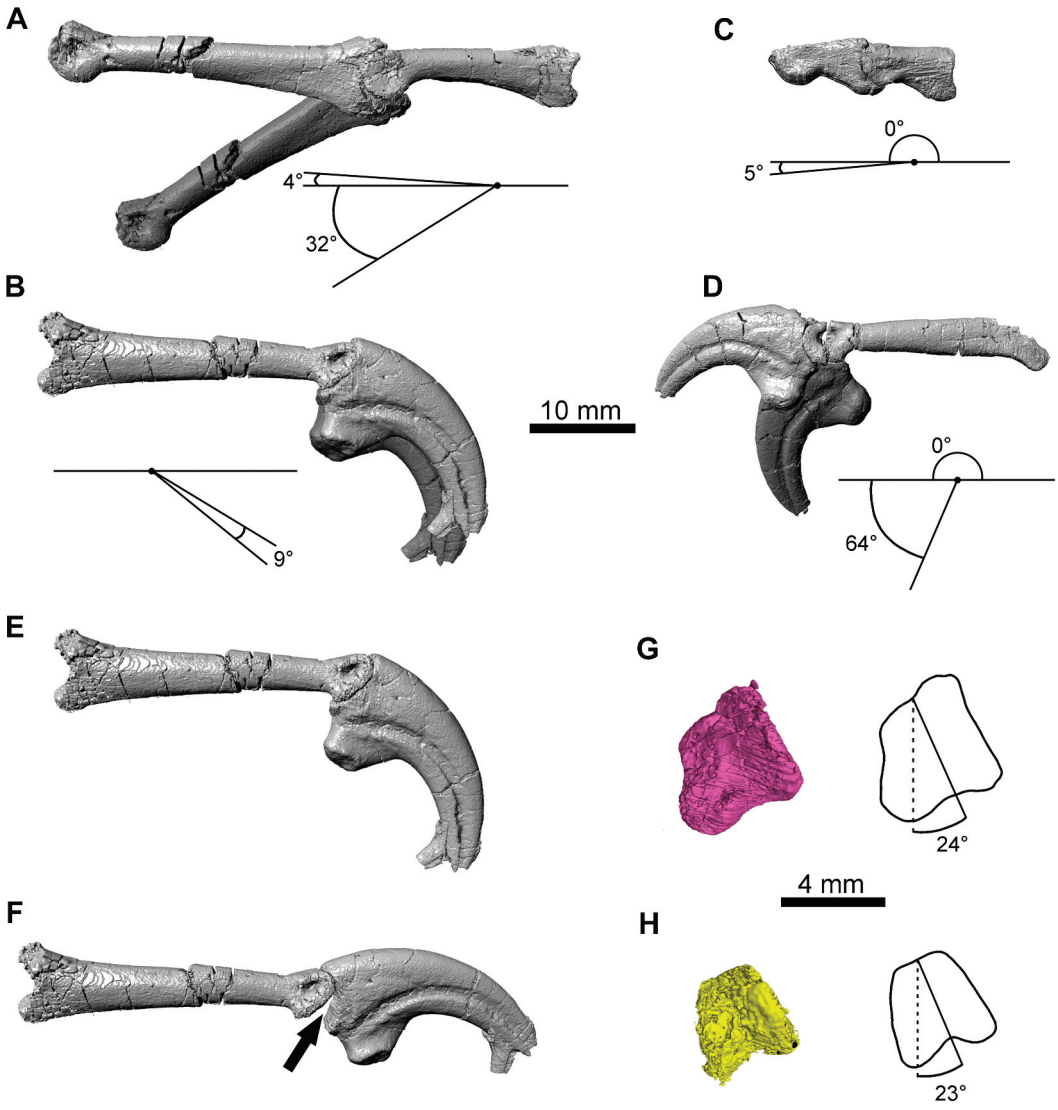

Figure 5. Ranges of motion of manual phalanges of SDUST-V1042. (A), manual phalanx II-1 and II-2; (B), manual phalanx II-2 and II-3; (C), manual phalanx III-1 and III-2; (D), manual phalanx III-3 and III-4; (E-F), casts of phalanx II-2 and II-3 of SDUST-V1042 in various positions, showing that the ungual becomes disarticulated when extended; (G-H), the manual phalanges are twisted, (G) distal view of phalanx II-1, (H) distal view of phalanx III-3.

to that of digit II. In compsognathids such as *Beipiaognathus jii* (Hu et al. 2016) and *Sinocalliopteryx gigas* (Ji et al. 2007), manual phalanx III-3 is shorter than phalanges III-1 and III-2 combined and the flexor tubercles are weakly developed, but phalanx III-3 is longer than phalanges III-1 and III-2 combined and the flexor tubercles are well developed in SDUST-V1042. In ornithomimosaurians such as *Shenzhousaurus orientalis* (Ji et al. 2003) and therizinosauroids such as *Beipiaosaurus inexpectus* (Xu et al. 1999a), *Jianchangosaurus yixianensis* (Pu et al. 2013) and *Lingyuanosaurus sihedangensis* (Yao et al. 2019), flexor tubercles of these groups are small, and not as high as that of the proximal articular facet, but in SDUST-V1042, the flexor tubercles are well developed and the height is similar to that of the proximal articular facet. In oviraptorosaurians, the manus is well preserved in *Caudipteryx* spp. while the manus of *Similicaudipteryx yixianensis* (He et al. 2008) and *Xingtianosaurus ganqi* (Qiu et al. 2019) are incompletely preserved. In *Caudipteryx* spp. (Ji et al. 1998; Zhou and Wang 2000), the phalangeal formula is 2-3-2, but in SDUST-V1042, the phalangeal formula is 2-3-4. In dromaeosaurids such as *Microraptor zhaoianus* (Xu et al. 2000, 2003; Gong et al. 2012; Pei et al. 2014) and *Sinornithosaurus millenii* (Xu et al. 1999b), manual phalanx III-1 is more than twice the length of phalanx III-2, and the phalanges of the third digit are much slenderer than those of the second digit, which is clearly distinguished from SDUST-V1042 in which both phalanges III-1 and III-2 are subequal in length, and phalanges of the second digit are almost as robust as those of the third digit. SDUST-V1042 also is different from the basal avialans. In jeholornithiforms such as *Jeholornis prima* (Zhou and Zhang 2002) and *Kompsornis longicaudus* (Wang et al. 2020), the transverse width of phalanx II-1 is approximately 2 times that of phalanx II-2, while in SDUST-V1042, phalanx II-1 is only slightly thicker than II-2. In sapeornithids such as *Sapeornis angustis* (Pauline et al. 2009) and *Sapeornis chaoyangensis* (Gao et al. 2012b), the phalangeal formula is 2-3-2, but in SDUST-V1042, the phalangeal formula is 2-3-4. In confuciusornithids such as *Confuciusornis sanctus* (Dalsätt et al. 2006) and *Eoconfuciusornis zhengi* (Zhang et al. 2008), phalanx I-2 is the largest, phalanx III-4 is intermediate and phalanx II-3 is the smallest, unlike in SDUST-V1042 phalanx II-3 is larger than phalanx III-4.

As aforementioned, the manual morphology of SDUST-V1042 is different from other theropod groups of the Jehol Biota, but

shows shared features with previously reported early-diverging troodontids of the Jehol Biota. Therefore, SDUST-V1042 was inferred as an early-diverging troodontid.

Range of motion

The ROM of phalanges I-2, II-2, II-3, III-2, III-3, III-4 are measured with Maya (Figure 5). Only the approximate degree of flexion of phalanges I-2 and III-3 are measured due to the incompletely preserved joints. As in ornithomimosaurians, oviraptorosaurians and dromaeosaurids, SDUST-V1042 exhibits a significant reduction of the range of the manual extension, but has a relatively large range of flexion.

In SDUST-V1042, the ROM of phalanx I-2 is about 71° for flexion. In digit II, phalanx II-1 could be twisted along its long axis by 24° (Figure 5g), so that the distal phalanges of the second digit converge medially during flexion. The ROM of phalanx II-2 is from 32° for flexion to 4° for extension (Figure 5a). Phalanx II-3 exhibits a permanent state of flexion, and has a 9° range of movement at the joint between phalanges II-2 and II-3 (Figure 5b). The flat distal articular end of phalanx II-2 strongly hinders the extension of phalanx II-3 (Figure 5e, f).

In digit III, phalanx III-2 is nearly immobile, with a merely 5° for flexion (Figure 5c). Phalanx III-3 is about 18° for flexion and can be twisted along its long axis by 23° (Figure 5h), so that phalanx III-4 also converges medially during flexion. Phalanx III-4 shows a high capability of flexion, with a maximum range of 64° for flexion, but lacks capability of hyperextension (Figure 5d). The large range of flexion of phalanx III-4 is also present in *Deinonychus antirrhopus* (Senter 2006b).

Discussion

Manual morphology of troodontids

In most troodontids, the manual phalanges are only simply described, and detailed morphological descriptions are limited to *Sinornithoides youngi* (Currie and Dong 2001), *Urbacodon* sp. (Averianov and Sues 2016) and the unnamed troodontid MPC-D 100/140 (Tsuihiji et al. 2016). In this study, SDUST-V1042 reveals several new manual features for the troodontids, such as the asymmetrical articular facets (the lateral is larger than medial) of phalanges II-1 and II-2, the shafts of phalanx II-1 and phalanx III-3 twisted medially, the ventral side of the distal end of phalanx II-2 flat and the proximal articular surface of phalanx III-1 non-trochoid. These features are reported in troodontids for the first time, but some of these features are also distributed in dromaeosaurids and other theropod groups (e.g. *Herrerasaurus ischigualastensis*, allosauroids, compsognathids and oviraptorosaurians).

In particular, the asymmetrical articular facets between phalanx II-1 and phalanx II-2 are known in dromaeosaurids like *Deinonychus antirrhopus* (Ostrom 1969) and *Velociraptor mongoliensis* (Norell and Makovicky 1999). In contrast, the symmetrical condition is present in other theropods such as the oviraptorosaurian *Hagryphus giganteus* (Zanno and Sampson 2005). Furthermore, the distal end of phalanx II-1 is asymmetrical and medially twisted (Figure 3g), and this condition may lead to the medial converging of digit II during flexion. The twisted shaft of phalanx II-1 is reported in *Herrerasaurus ischigualastensis* (Sereno 1993), but its shaft is laterally twisted. Moreover, the medially twisted shaft of phalanx III-3 is known in *Bambiraptor feinbergi* (Senter 2006b). Its shaft is twisted about 35° (estimated from Senter 2006b, figure 4aa), slightly stronger than that in SDUST-V1042 (23°). This twisting enables ungual III approaching digit II during flexion.

In SDUST-V1042, the ventral side of the distal end of phalanx II-2 is flat, limiting the movement of phalanx II-3. This condition is also present in the allosauroids *Acrocanthosaurus atokensis* (Senter and Robins 2005) and *Sinraptor dongi* (Currie and Zhao 1993) and the compsognathid *Compsognathus longipes* (Gishlick and Gauthier 2007). In contrast, in most theropods, the distal end of penultimate phalanges is rounded, allowing the ungual more freedom of movement (Senter and Robins 2005). Moreover, in SDUST-V1042, the proximal articular surface of phalanx III-1 is undivided and non-trochoid, so that phalanx III-1 could move somewhat horizontally, as in *Acrocanthosaurus atokensis* (Senter and Robins 2005), *Chirostenotes pergracilis* (Currie and Russell 1988) and *Deinonychus antirrhopus* (Ostrom 1969), but unlike *Bambiraptor feinbergi* (Senter 2006b) and *Velociraptor mongoliensis* (Norell and Makovicky 1999).

The changes of manual ROM and function in theropods

The ROM of the manus has been studied widely in theropods such as allosauroids, tyrannosauroids, ornithomimosaurians, oviraptorosaurian and dromaeosaurids (Carpenter 2002; Kobayashi and Barsbold 2005; Senter and Parrish 2005; Senter and Robins 2005; Senter 2006a, 2006b; White et al. 2015; Senter and Sullivan 2019) (Table 1). Generally, three types of manual joints exist: the metacarpophalangeal joint (proximal to I-1, II-1 and III-1), the interphalangeal joint (proximal to II-2, III-2 and III-3) and the ungual joint (proximal to I-2, II-3 and III-4).

As for the metacarpophalangeal joints, the ranges of motion vary largely. For metacarpophalangeal joint I, the extension ranges from 5° (*Chirostenotes pergracilis*, Senter and Parrish 2005) to 90° (*Acrocanthosaurus atokensis*, Senter and Robins 2005), while the flexion ranges between 10° (*Australovenator wintonensis*, White et al. 2015) and 70° (*Harpymimus okladnikovi*, Kobayashi and Barsbold 2005). For metacarpophalangeal joint II, the extension ranges from 10° (*Deinonychus antirrhopus*, Senter 2006b) to 105° (*Dilophosaurus wetherilli*, Senter and Sullivan 2019), while the flexion ranges between 18° (*Allosaurus fragilis*, Senter and Parrish 2005) and 51° (*Deinonychus antirrhopus*, Senter 2006b).

As for the interphalangeal joints, especially in digit II, they appear to have wide ranges from 31° to 75° for flexion. A high capability of extension (>35°) is present in the allosauroids such as *Acrocanthosaurus atokensis* (Senter and Robins 2005) and in the tyrannosauroids such as *Australovenator wintonensis* (White et al. 2015). However, a low extension condition (<15°) is present in the ornithomimosaurians and pennaraptorans (e.g. *Harpymimus okladnikovi*, Senter and Parrish 2005; *Bambiraptor feinbergi* and *Deinonychus antirrhopus*; Senter 2006b), except phalanx II-2 of *Chirostenotes pergracilis* (Senter and Parrish 2005).

As for the ungual joints, the ranges of flexion are mostly larger than 35°, except phalanx I-2 of *Tyrannosaurus rex* (Senter and Parrish 2005) and phalanx II-3 of *Dilophosaurus wetherilli* (Senter and Sullivan 2019) and *Guanlong wucaii* (Yu et al. 2015), but the ranges of extension of the ungual joints vary. In the tyrannosauroid *Australovenator wintonensis* (White et al. 2015), the ranges of extension are large (>35°), but in the allosauroid *Acrocanthosaurus atokensis* (Senter and Robins 2005) and ornithomimosaurians, the unguals are permanent in flexion. In the pennaraptorans (e.g. *Chirostenotes pergracilis*, Senter and Parrish 2005; *Bambiraptor feinbergi* and *Deinonychus antirrhopus*, Senter 2006b), the ranges of extension are limited (<10°).

Interestingly, in relatively early-diverging theropods such as *Dilophosaurus wetherilli*, allosauroids and tyrannosauroids, all metacarpophalangeal joints (as well as some other joints) show larger range of extension than flexion. As a contrast, almost all manual joints show larger range of flexion than extension in *Coelophysis*

Table 1. Range of motion (ROM) values of various theropods and SDUST-V1042 (Senter and Parrish 2005; Senter and Robins 2005; Senter 2006a, 2006b; White et al. 2015; Yu et al. 2015; Senter and Sullivan 2019).

Dinosaur taxon		I-1	I-2	II-1	II-2	II-3	III-1	III-2	III-3	III-4
Coelophysis bauri	Extension	18	26	17	13	10	?	?	?	?
	Flexion	54	40	48	60	50	?	?	?	?
	ROM	72	66	65	73	60	?	?	?	?
Dilophosaurus wetherilli	Extension	19	28	105	?	18	85	31	18	5
	Flexion	16	65	21	?	27	62	53	62	47
	ROM	35	93	126	?	45	147	84	80	52
Allosaurus fragilis	Extension	55	?	20	10	0	?	?	?	?
	Flexion	19	?	18	63	58	?	?	?	?
	ROM	74	?	38	73	58	?	?	?	?
Acrocanthosaurus atokensis	Extension	90	−116	77	97	−98	73	18	20	0
	Flexion	35	119	36	70	133	11	28	50	108
	ROM	125	3	113	167	35	84	46	70	108
Australovenator wintonensis	Extension	40	42	38	37	37	?	?	?	50
	Flexion	10	80	36	31	73	?	?	?	62
	ROM	50	122	72	68	110	?	?	?	112
Tyrannosaurus rex	Extension	35	34	?	?	?	?	?	?	?
	Flexion	18	22	?	?	?	?	?	?	?
	ROM	53	56	?	?	?	?	?	?	?
Guanlong wucaii	Extension	49	10	46	22	28	17	30	26	18
	Flexion	31	71	31	72	33	11	14	53	70
	ROM	80	81	77	94	61	28	44	79	88
Harpymimus okladnikovi	Extension	28	0	19	14	0	?	?	?	?
	Flexion	70	97	25	46	90	?	?	?	?
	ROM	98	97	44	60	90	?	?	?	?
Ornitholestes hermanni	Extension	29	0	?	?	17	?	?	?	?
	Flexion	52	85	?	?	100	?	?	?	?
	ROM	81	85	?	?	117	?	?	?	?
Gallimimus sp.	Extension	20	0	25	0	0	?	?	?	?
	Flexion	33	96	27	33	90	?	?	?	?
	ROM	53	96	52	33	90	?	?	?	?
Chirostenotes pergracilis	Extension	5	7	24	25/16	4	?	?	?	?
	Flexion	51	62	41	58/60	52	?	?	?	?
	ROM	56	69	65	83/76	56	?	?	?	?
Bambiraptor feinbergi	Extension	15	0	28	7	6	−4	10	−2	?
	Flexion	51	76	50	70	92	36	36	37	?
	ROM	66	76	78	77	98	32	46	35	?
Deinonychus antirrhopus	Extension	43	4	10	0	11	23	−11	0	11
	Flexion	49	70	51	75	85	22	62	9	74
	ROM	92	74	61	75	96	45	51	9	85
SDUST-V1042	Extension	?	?	?	4	−30	?	0	?	0
	Flexion	?	~71	?	32	39	?	5	~18	64
	ROM	?	?	?	36	9	?	5	?	64

'?' represents the measurements are unavailable, '~' represents the estimated value.

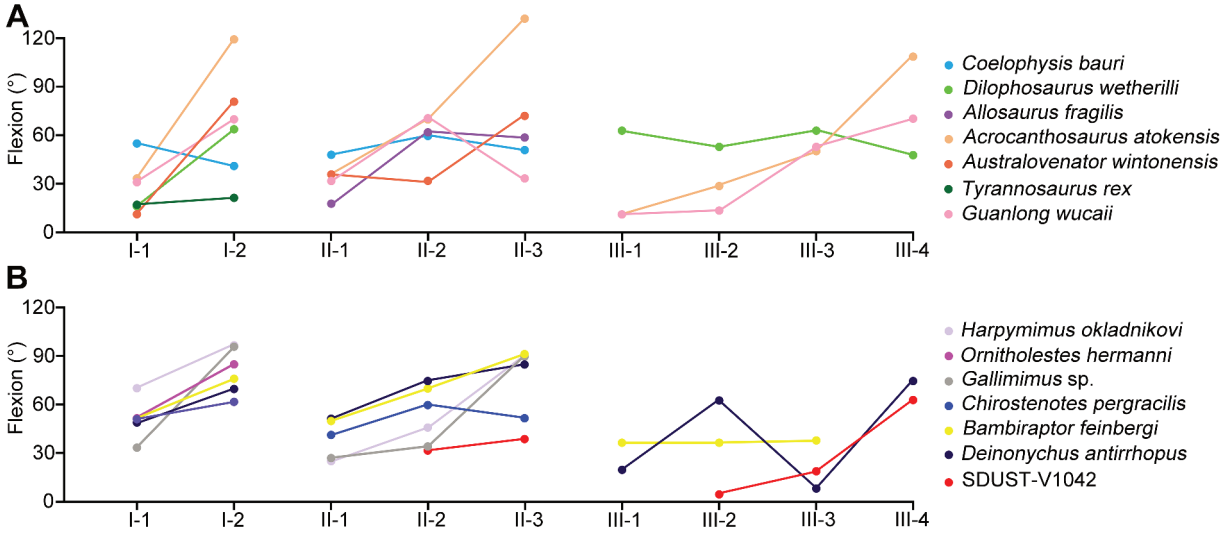

Figure 6. Ranges of flexion within the same digit in relatively early-diverging theropods (A) and maniraptoriforms (B).

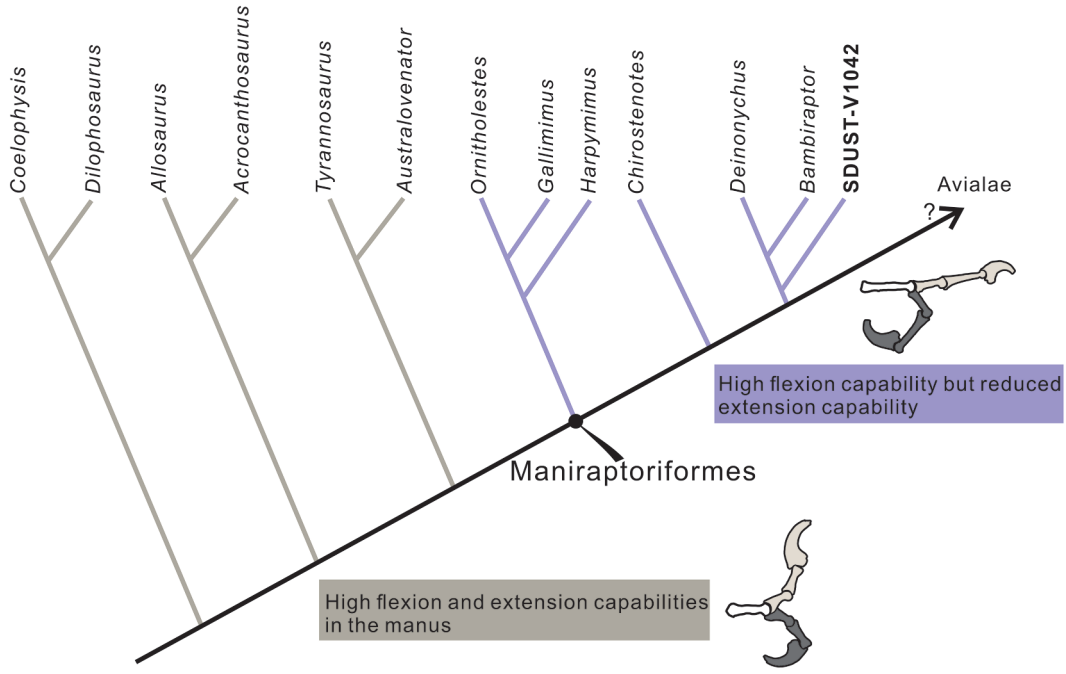

Figure 7. The evolutionary trend of the manual ROM along the simplified phylogenetic tree of theropods. The phylogeny was created with reference to previous studies of the manual ROM (Senter and Parrish 2005; Senter and Robins 2005; White et al. 2015).

bauri and maniraptoriforms (Table 1). Moreover, a trend of the increase of ranges of flexion from the proximal to the distal phalanges within the same digit, which may be associated with the grasping ability of the manus, is likely present in tetanurans with some exceptions such as in the second digit of *Allosaurus fragilis, Australovenator wintonensis* and *Guanlong wucaii* (Figure 6). This pattern becomes more stable in Maniraptoriformes with only few exceptions such as digit II of *Chirostenotes pergracilis* and digit III of *Deinonychus antirrhopus* (Figure 6).

In summary, the manus exhibits considerable hyperextension as a primitive condition of theropod dinosaurs as in coelophysoids, allosauroids and tyrannosauroids (White et al. 2015), while a significant reduction of the manual hyperextension occurs in ornithomimosaurians, oviraptorosaurians and dromaeosaurids (Figure 7). Generally, there is a tendency to decrease in the capability of manual extension in these theropods (White et al. 2015; Yu et al. 2015). In SDUST-V1042, the capability of the manual extension is obviously low, further supporting this tendency from early-diverging theropods to maniraptoriforms.

The decrease of the capability of the manual extension in theropods is likely associated with the change of the manual function. For example, in the tyrannosauroid *Australovenator wintonensis* (White et al. 2015), the range of hyperextension of the manual unguals is large and this kind of animals possibly possesse a unique manual function associated with predation. In dromaeosaurids, the range of hyperextension has been significantly reduced, even though the range of flexion remains large. This condition shows that compared with early-diverging forms, dromaeosaurids were more likely to use their manus to grasp, while the dispatch could be achieved orally or with the sickle-like claw on its second pedal digit (Ostrom 1969; Manning et al. 2009; White et al. 2015). As in dromaeosaurids, SDUST-V1042 also shows large range for flexion and limited range for extension, which suggests that it may also try to use its manus to grasp like dromaeosaurids. In extant primates, the manus also have large range for flexion and limited range for extension, and the prehension of objects by hand is integral (Fragaszy and Crast 2016).

Conclusions

We described a right manus of a recently discovered specimen SDUST-V1042 from the Jehol Biota of western Liaoning, China, which is inferred as an early-diverging troodontid. This specimen reveals new manual features like both ends of phalanx II-1 and phalanx II-2 asymmetrical, phalanx II-1 and phalanx III-3 medially twisted, the ventral side of the distal end of phalanx II-2 flat and the proximal articular surface of phalanx III-1 is not trochoid. The ROM analysis of this manus shows that the range of flexion is relatively large while the range of extension is relatively limited in this troodontid, consistent with the tendency of the decrease of the manual extension capabilities from early-diverging theropods to maniraptoriforms.

Acknowledgments

We would like to thank Qin-Fang Fang (China University of Geosciences, Beijing) for his help with CT scanning of the specimen. We thank Dr Shu-An Ji (Institute of Geology, Chinese Academy of Geological Sciences, Beijing) and two anonymous reviewers for their reviews.

Disclosure statement

No potential conflict of interest was reported by the author(s).

Funding

This work was supported by the National Natural Science Foundation of China [41972025; 41688103; 42161134003]; Taishan Scholar Program of Shandong Province [tsqn201812070]; Program for Innovative Research Team of Excellent Talents in University of Shandong Province [2019KJH004]; Scientific Research Foundation of Shenyang Normal University, China [BS202207]; International Partnership Program of Chinese Academy of Sciences [132311KYSB20190010, 132311KYSB20180016].

References

Agnolin FL, Motta MJ, Egli FB, Coco GL, Novas FE. 2019. Paravian phylogeny and the dinosaur-bird transition: an overview. Front Earth Sci. 6:1–28. accessed 2019 Feb 12. doi:10.3389/feart.2018.00252.

Averianov A, Sues HD. 2016. Troodontidae (Dinosauria: Theropoda) from the Upper Cretaceous of Uzbekistan. Cretac Res. 59:98–110. accessed 2015 Nov 27. doi:10.1016/j.cretres.2015.11.005.

Barsbold R, Osmólska H, Kurzanov SM. 1987. On a new troodontid (Dinosauria, Theropoda) from the Early Cretaceous of Mongolia. Acta Palaeontol Pol. 32(1–2):121–132.

Carpenter K. 2002. Forelimb biomechanics of nonavian theropod dinosaurs in predation. Senckenb Lethaea. 82(1):59–75. doi:10.1007/BF03043773.

Currie PJ, Dong ZM. 2001. New information on Cretaceous troodontids (Dinosauria, Theropoda) from the People's Republic of China. Can J Earth Sci. 38(12):1753–1766. doi:10.1139/e01-065.

Currie PJ, Russell DA. 1988. Osteology and relationships of *Chirostenotes pergracilis* (Saurischia, Theropoda) from the Judith River (Oldman) Formation of Alberta, Canada. Can J Earth Sci. 25(7):972–986. doi:10.1139/e88-097.

Currie PJ, Zhao XJ. 1993. A new carnosaur (Dinosauria, Theropoda) from the Jurassic of Xinjiang, People's Republic of China. Can J Earth Sci. 30(10–11):2037–2081. doi:10.1139/e93-179.

Dalsätt J, Zhou ZH, Zhang FC, Ericson PGP. 2006. Food remains in *Confuciusornis sanctus* suggest a fish diet. Naturwissenschaften. 93 (9):444–446. doi:10.1007/s00114-006-0125-y.

Evans DC, Cullen TM, Larson DW, Rego A. 2017. A new species of troodontid theropod (Dinosauria: Maniraptora) from the Horseshoe Canyon Formation (Maastrichtian) of Alberta, Canada. Can J Earth Sci. 54(8):813–826. doi:10.1139/cjes-2017-0034.

Fragaszy DM, Crast J. 2016. Functions of the hand in primates. In: Kivell TL, Lemelin P, Richmond BG, Schmitt D, editors. The Evolution of the Primate Hand. New York (NY): Springer; p. 313–344.

Galton PM. 1971. Manus movements of the coelurosaurian dinosaur *Syntarsus* and opposability of the theropod hallux. Arnoldia. 5(15):1–8.

Gao CL, Chiappe LM, Zhang FJ, Pomeroy DL, Shen CZ, Chinsamy A, Walsh MO. 2012b. A subadult specimen of the Early Cretaceous bird *Sapeornis chaoyangensis* and a taxonomic reassessment of sapeornithids. J Vertebr Paleontol. 32(5):1103–1112. doi:10.1080/02724634.2012.693865.

Gao CL, Morschhauser EM, Varricchio DJ, Liu JY, Zhao B, Farke AA. 2012a. A second soundly sleeping dragon: new anatomical details of the Chinese troodontid *Mei long* with implications for phylogeny and taphonomy. PLoS ONE. 7(9:)e45203. accessed 2012 Sept 27. doi:10.1371/journal.pone.0045203.

Gishlick AD. 2001. The function of the manus and forelimb of *Deinonychus antirrhopus* and its importance for the origin of avian flight. In: Gauthier J, Gall LF, editors. New Perspectives on the Origin and Early Evolution of Birds. New Haven (CT): Yale Peabody Museum; p. 301–318.

Gishlick AD, Gauthier JA. 2007. On the manual morphology of *Compsognathus longipes* and its bearing on the diagnosis of Compsognathidae. Zool J Linn Soc. 149(4):569–581. doi:10.1111/j.1096-3642.2007.00269.x.

Gong EP, Martin LD, Burnham DA, Falk AR, Hou LH. 2012. A new species of *Microraptor* from the Jehol Biota of northeastern China. Palaeoworld. 21 (2):81–91. doi:10.1016/j.palwor.2012.05.003.

He T, Wang XL, Zhou ZH. 2008. A new genus and species of caudipterid dinosaur from the Lower Cretaceous Jiufotang Formation of western Liaoning, China. Vertebr PalAsiat. 46(3):178–189.

Hu YC, Wang XR, Huang JD. 2016. A new species of compsognathid from the Early Cretaceous Yixian Formation of western Liaoning, China. J Geol. 40 (2):191–196. doi:10.3969/j.issn.1674-3636.2016.02.191.

Ji Q, Currie PJ, Norell MA, Ji SA. 1998. Two feathered dinosaurs from northeastern China. Nature. 393(6687):753–761. doi:10.1038/31635.

Ji SA, Ji Q. 2007. *Jinfengopteryx* compared to *Archaeopteryx*, with comments on the mosaic evolution of long-tailed avialan birds. Acta Geol Sin-Engl. 81 (3):337–343. doi:10.1111/j.1755-6724.2007.tb00957.x.

Ji SA, Ji Q, JC L, Yuan CX. 2007. A new giant compsognathid dinosaur with long filamentous integuments from Lower Cretaceous of northeastern China. Acta Geol Sin-Engl. 81(1):8–15.

Ji Q, Ji SA, Lü JC, You HL, Chen W, Liu YQ, Liu YX. 2005. First avialian bird from China (*Jinfengopteryx elegans* gen. et sp. nov.). Geol Bull China. 24 (3):197–210.

Ji Q, Norell MA, Makovicky PJ, Gao KQ, Ji SA, Yuan CX. 2003. An early ostrich dinosaur and implications for ornithomimosaur phylogeny. Am Mus Novit. 3420:1–19. doi:10.1206/0003-0082(2003)420<0001:AEODAI>2.0.CO;2

Kobayashi K, Barsbold R. 2005. Anatomy of *Harpymimus okladnikovi* Barsbold and Perle 1984 (Dinosauria; Theropoda) of Mongolia. In: Carpenter K, editor. The Carnivorous Dinosaurs. Bloomington (IL): Indiana University Press; p. 97–126.

Makovicky PJ, Norell MA. 2004. Troodontidae. In: Weishampel DB, Dodson P, Osmólska H, editors. The Dinosauria. 2nd ed. Berkeley: University of California Press; p. 184–195.

Manning PL, Margetts L, Johnson MR, Withers PJ, Sellers WI, Falkingham PL, Mummery PM, Barrett PM, Raymont DR. 2009. Biomechanics of dromaeosaurid dinosaur claws: application of X-ray microtomography, nanoindentation, and finite element analysis. Anat Rec. 292(9):1397–1405. doi:10.1002/ar.20986.

Norell MA, Makovicky PJ. 1999. Important features of the dromaeosaurid skeleton II: information from newly collected specimens of *Velociraptor mongoliensis*. Am Mus Novit. 3282:1–45.

Norell MA, Makovicky PJ, Clark JM. 2000. A new troodontid theropod from Ukhaa Tolgod, Mongolia. J Vertebr Paleontol. 20(1):7–11. doi:10.1671/0272-4634(2000)020[0007:ANTTFU]2.0.CO;2.

Osmólska H, Roniewicz E. 1969. Deinocheiridae, a new family of theropod dinosaurs. Palaeontol Pol. 21:5–19.

Ostrom JH. 1969. Osteology of *Deinonychus antirrhopus*, an unusual theropod from the Lower Cretaceous of Montana. Bull Peabody Mus Nat Hist. 30:1–165.

Pauline P, Zhou ZH, Zhang FC. 2009. A new species of the basal bird *Sapeornis* from the Early Cretaceous of Liaoning, China. Vertebr PalAsiat. 47 (3):194–207.

Pei R 2015. New paravian fossils from the Mesozoic of East Asia and their bearing on the phylogeny of the Coelurosauria [dissertation]. New York (NY): Columbia University.

Pei R, Li QG, Meng QJ, Gao KQ, Norell MA. 2014. A new specimen of *Microraptor* (Theropoda: Dromaeosauridae) from the Lower Cretaceous of western Liaoning, China. Am Mus Novit. 3821:1–28. doi:10.1206/3821.1

Pei R, Li QG, Meng QJ, Norell MA, Gao KQ. 2017b. New specimens of *Anchiornis huxleyi* (Theropoda: Paraves) from the Late Jurassic of northeastern China. Bull Am Mus Nat Hist. 411:1–67. doi:10.1206/0003-0090-411.1.1

Pei R, Norell MA, Barta DE, Bever GS, Pittman M, Xu X. 2017a. Osteology of a new Late Cretaceous troodontid specimen from Ukhaa Tolgod, Ömnögovi Aimag, Mongolia. Am Mus Novit. 3889:1–47. doi:10.1206/3889.1

Pei R, Qin YY, Wen AS, Zhao Q, Wang Z, Liu ZM, Guo WLS, Liu P, Ye WM, Wang LY, et al. 2022. A new troodontid from the Upper Cretaceous Gobi Basin of Inner Mongolia, China. Cretac Res. 130:105052. accessed 2021 Oct 1. doi:10.1016/j.cretres.2021.105052.

Pu HY, Kobayashi Y, JC L, Xu L, Wu YH, Chang HL, Zhang JM, Jia SH, Claessens L. 2013. An unusual basal therizinosaur dinosaur with an ornithischian dental arrangement from northeastern China. PLoS ONE. 8 (5)e63423. accessed 2013 May 29. doi:10.1371/journal.pone.0063423.

Qiu R, Wang XL, Wang Q, Li N, Zhang JL, Ma YY. 2019. A new caudipterid from the Lower Cretaceous of China with information on the evolution of the manus of Oviraptorosauria. Sci Rep. 9(1)accessed 2019 Apr 25:6431. doi:10.1038/s41598-019-42547-6.

Rauhut OWM, Foth C. 2020. The origin of birds: current consensus, controversy, and the occurrence of feathers. In: Foth C, Rauhut OWM, editors. The Evolution of Feathers. Cham (Switzerland): Springer; p. 27–45.

Russell DA, Dong ZM. 1993. A nearly complete skeleton of a new troodontid dinosaur from the Early Cretaceous of the Ordos Basin, Inner Mongolia, People's Republic of China. Can J Earth Sci. 30(10–11):2163–2173. doi:10.1139/e93-187.

Senter P. 2006a. Forelimb function in *Ornitholestes hermanni* Osborn (Dinosauria, Theropoda). Palaeontology. 49:1029–1034. doi:10.1111/j.1475-4983.2006.00585.x.

Senter P. 2006b. Comparison of forelimb function between *Deinonychus* and *Bambiraptor* (Theropoda: Dromaeosauridae). J Vertebr Paleontol. 26 (4):897–906. doi:10.1671/0272-4634(2006)26[897:COFFBD]2.0.CO;2.

Senter P, Parrish JM. 2005. Functional analysis of the hands of the theropod dinosaur *Chirostenotes pergracilis*: evidence for an unusual paleoecological role. PaleoBios. 25(2):9–19.

Senter P, Robins JH. 2005. Range of motion in the forelimb of the theropod dinosaur *Acrocanthosaurus atokensis*, and implications for predatory behaviour. J Zool Lond. 266(3):307–318. doi:10.1017/S0952836905006989.

Senter PJ, Sullivan C. 2019. Forelimbs of the theropod dinosaur *Dilophosaurus wetherilli*: range of motion, influence of paleopathology and soft tissues, and description of a distal carpal bone. Palaeontol Electron. 22(2.30A)accessed 2019 Jun 5:1–19. doi:10.26879/900.

Sereno PC. 1993. The pectoral girdle and forelimb of the basal theropod *Herrerasaurus ischigualastensis*. J Vertebr Paleontol. 13(4):425–450. doi:10.1080/02724634.1994.10011524.

Shen CZ, Lü JC, Liu SZ, Martin K, Stephen LB, Gao HL. 2017a. A new troodontid from the Lower Cretaceous Yixian Formation of Liaoning Province, China. Acta Geol Sin-Engl. 91(3):763–780. doi:10.1111/1755-6724.13307.

Shen CZ, Zhao B, Gao CL, Lü JC, Martin K. 2017b. A new troodontid dinosaur (*Liaoningvenator curriei* gen. et sp. nov.) from the Early Cretaceous Yixian

Formation in western Liaoning Province. Acta Geosci Sin. 38(3):359–371. doi:10.3975/cagsb.2017.03.06.
Tsuihiji T, Barsbold R, Watabe M, Tsogtbaatar K, Chinzorig T, Fujiyama Y, Suzuki S. 2014. An exquisitely preserved troodontid theropod with new information on the palatal structure from the Upper Cretaceous of Mongolia. Naturwissenschaften. 101(2):131–142. doi:10.1007/s00114-014-1143-9.
Tsuihiji T, Barsbold R, Watabe M, Tsogtbaatar K, Suzuki S, Hattori S. 2016. New material of a troodontid theropod (Dinosauria: Saurischia) from the Lower Cretaceous of Mongolia. Hist Biol. 28(1–2)accessed 2015 Oct 1:128–138. doi:10.1080/08912963.2015.1005086.
Wang XR, Huang JD, Kundrát M, Cau A, Liu XY, Wang Y, Ju SB. 2020. A new jeholornithiform exhibits the earliest appearance of the fused sternum and pelvis in the evolution of avialan dinosaurs. J Asian Earth Sci. 199:104401. accessed 2020 May 23. doi:10.1016/j.jseaes.2020.104401.
White MA, Bell PR, Cook AG, Barnes DG, Tischler TR, Bassam BJ, Elliott DA, Carrier D. 2015. Forearm range of motion in *Australovenator wintonensis* (Theropoda, Megaraptoridae). PLoS ONE. 10(9): e0137709. accessed 2015 Sept 14. doi: 10.1371/journal.pone.0137709.
Xu X, Currie P, Pittman M, Xing LD, Meng QJ, Lü JC, Hu DY, Yu CY. 2017. Mosaic evolution in an asymmetrically feathered troodontid dinosaur with transitional features. Nat Commun. 8:14972. accessed 2017 May 2. doi:10.1038/ncomms14972.
Xu X, Norell MA. 2004. A new troodontid dinosaur from China with avian-like sleeping posture. Nature. 431(7010):838–841. doi:10.1038/nature02898.
Xu X, Norell MA, Kuang XW, Wang XL, Zhao Q, Jia CK. 2004. Basal tyrannosauroids from China and evidence for protofeathers in tyrannosauroids. Nature. 431(7009):680–684. doi:10.1038/nature02855.
Xu X, Norell MA, Wang XL, Makovicky PJ, Wu XC. 2002. A basal troodontid from the Early Cretaceous of China. Nature. 415(6873):780–784. doi:10.1038/415780a.
Xu X, Tang ZL, Wang XL. 1999a. A therizinosauroid dinosaur with integumentary structures from China. Nature. 399(6734):350–354. doi:10.1038/20670.
Xu X, Tan QW, Sullivan C, Han FL, Xiao D, Farke AA. 2011. A short-armed troodontid dinosaur from the Upper Cretaceous of Inner Mongolia and its implications for troodontid evolution. PLoS ONE. 6(9):e22916. accessed 2011 Sept 7. doi:10.1371/journal.pone.0022916.
Xu X, Wang XL. 2004. A new troodontid (Theropoda: Troodontidae) from the Lower Cretaceous Yixian Formation of western Liaoning, China. Acta Geol Sin-Engl. 78(1):22–26. doi:10.1111/j.1755-6724.2004.tb00671.x.
Xu X, Wang XL, Wu XC. 1999b. A dromaeosaurid dinosaur with a filamentous integument from the Yixian Formation of China. Nature. 401 (6750):262–266. doi:10.1038/45769.
Xu X, Wang KB, Zhang K, Ma QY, Xing LD, Sullivan C, Hu DY, Cheng SQ, Wang S. 2012. A gigantic feathered dinosaur from the Lower Cretaceous of China. Nature. 484(7392):92–95. doi:10.1038/nature10906.
Xu X, Zhou ZH, Wang XL. 2000. The smallest known non-avian theropod dinosaur. Nature. 408(6813):705–708. doi:10.1038/35047056.
Xu X, Zhou ZH, Wang XL, Kuang XW, Zhang FC, Du XK. 2003. Four-winged dinosaurs from China. Nature. 421(6921):335–340. doi:10.1038/nature01342.
Yao X, Liao CC, Sullivan C, Xu X. 2019. A new transitional therizinosaurian theropod from the Early Cretaceous Jehol Biota of China. Sci Rep. 9(1):5026. accessed 2019 Mar 22. 10.1038/s41598-019-41560-z.
Yin YL, Pei R, Zhou CF. 2018. Cranial morphology of *Sinovenator changii* (Theropoda: Troodontidae) on the new material from the Yixian Formation of western Liaoning, China. PeerJ. 6:e4977. accessed 2018 Jun 20. doi:10.7717/peerj.4977.
Yu YL, Sullivan C, Xu X. 2015. Three-dimensional modeling of the manual digits of the theropod dinosaur *Guanlong*, with a preliminary functional analysis. Acta Palaeontol Sin. 54(2):165–173.
Zanno LE, Sampson SD. 2005. A new oviraptorosaur (Theropoda, Maniraptora) from the Late Cretaceous (Campanian) of Utah. J Vertebr Paleontol. 25 (4):897–904. doi:10.1671/0272-4634(2005)025[0897:ANOTMF]2.0.CO;2.
Zhang FC, Zhou ZH, Benton MJ. 2008. A primitive confuciusornithid bird from China and its implications for early avian flight. Sci China Ser D-Earth Sci. 51 (5):625–639. doi:10.1007/s11430-008-0050-3.
Zhou ZH, Wang XL. 2000. A new species of *Caudipteryx* from the Yixian Formation of Liaoning, Northeast China. Vertebr PalAsiat. 38(2):111–127.
Zhou ZH, Zhang FC. 2002. A long-tailed, seed-eating bird from the Early Cretaceous of China. Nature. 418(6896):405–409. doi:10.1038/nature00930.